# Quasistationary magnetic field generation with a laser-driven capacitor-coil assembly

V. T. Tikhonchuk,* M. Bailly-Grandvaux, and J. J. Santos
*Centre Lasers Intenses et Applications, University of Bordeaux-CNRS-CEA, 33405 Talence, France*

A. Poyé
*École Nationale Supérieure de Lyon, University Claude Bernard, CNRS, 69342 Lyon, France*
(Received 25 April 2017; published 14 August 2017)

Recent experiments are showing possibilities to generate strong magnetic fields on the excess of 500 T with high-energy nanosecond laser pulses in a compact setup of a capacitor connected to a single turn coil. Hot electrons ejected from the capacitor plate (cathode) are collected at the other plate (anode), thus providing the source of a current in the coil. However, the physical processes leading to generation of currents exceeding hundreds of kiloamperes in such a laser-driven diode are not sufficiently understood. Here we present a critical analysis of previous results and propose a self-consistent model for the high current generation in a laser-driven capacitor-coil assembly. It accounts for three major effects controlling the diode current: the space charge neutralization, the plasma magnetization between the capacitor plates, and the Ohmic heating of the external circuit—the coil-shaped connecting wire. The model provides the conditions necessary for transporting strongly super-Alfvenic currents through the diode on the time scale of a few nanoseconds. The model validity is confirmed by a comparison with the available experimental data.

DOI: 10.1103/PhysRevE.96.023202

## I. INTRODUCTION

Schemes of strong magnetic field generation with high-energy laser pulses provide a compact setup for plasma magnetohydrodynamic experiments in an open geometry accessible for various diagnostics. Differing from pulsed power sources of strong magnetic fields [1,2] evolving on a microsecond time scale and maintaining magnetic fields of an order of a few tens of tesla, the laser-driven sources operate on a nanosecond time scale and may create fields in vacuum exceeding hundreds of tesla.

Korobkin and Motylev [3] were the first to suggest using a laser for driving a current in a coil. With a relatively low energy (1 J) and long (20 ns) laser pulse, they measured an electric current of 2 kA, producing in the center of a 1.4-mm loop a magnetic field of 2 T. A possibility to upscale such a scheme was shown by Seely [4]. The first large energy experiment was reported by Daido *et al.* [5]. The authors used a single loop, 1-mm-diameter copper coil connected to two capacitor plates as schematically shown in Fig. 1. One plate (cathode) is irradiated by a laser pulse passing through a hole drilled in another plate (anode). In the experiment [5], the cathode was driven by a 1-ns 100-J pulse of a $CO_2$ laser at the wavelength of 10.6 $\mu$m. By using a loop antenna (B-dot probe) and extrapolating the data to the coil center, the authors reported a magnetic field of 40–60 T. They explained qualitatively that the current in the coil, attaining the value of 60 kA, is maintained by a high voltage of more than 200 kV generated in the capacitor by a thermoelectron emission from the laser-heated cathode. That is, the capacitor operates as a laser-driven diode. While no further details were provided concerning the target operation, it was mentioned that the maximum distance between the capacitor plates and thus the magnetic pulse duration are limited by the magnetization of the diode current.

Adaptation of this scheme for the Nd laser at the wavelength of 1.06 $\mu$m was reported by Courtois *et al.* [6]. The authors were using the Vulcan laser system with the pulse energy of 300 J and duration of 1 ns and generated a smaller magnetic field (up to 28 T) in a copper loop of a diameter of 2 mm with laser intensity of $4 \times 10^{16}$ W/cm$^2$. They studied the magnetic field dependence on the laser energy and pulse duration and compared single and double coil geometries, the latter allowing a better magnetic field homogeneity. The authors have discussed also difficulties in measuring the magnetic fields with coil probes positioned at a distance of a few tens of centimeters from the coil. First, extrapolation of the measured magnetic field and current to the coil position could be a source of a large error. Indeed, the dipole magnetic field decreases as a cube of the distance, and a difference between the coil size and the probe position of a factor of 100 implies a difference between the measured and estimated magnetic fields of 6 orders of magnitude. So even a small error in the measured field may result in the error of a factor of a few times in the coil. Moreover, the authors noticed that the current in the diode is also a source of an electromagnetic field, which could be of a compatible level and duration with the field generated in the coil. Because of proximity of the capacitor and the coil, it is difficult to make a clear distinction between the signals coming from these two sources. The detected magnetic field presents in fact a pulse in the gigahertz domain, which has to be separated from other parasite signals generated in such a harsh laser plasma interaction environment.

A major breakthrough in the development of capacitor-coil targets was presented by Fujioka *et al.* [7]. With a 1-kJ laser pulse of the Gekko laser system at wavelengths of 1.06 and 0.53 $\mu$m and 1-mm-diameter coils, the authors reported magnetic fields exceeding 1.5 kT, that is, by raising the laser pulse energy by a factor of 3, they achieved an increase of the magnetic induction by a factor of 50 compared to Ref. [6].

*tikhonchuk@u-bordeaux.fr

 

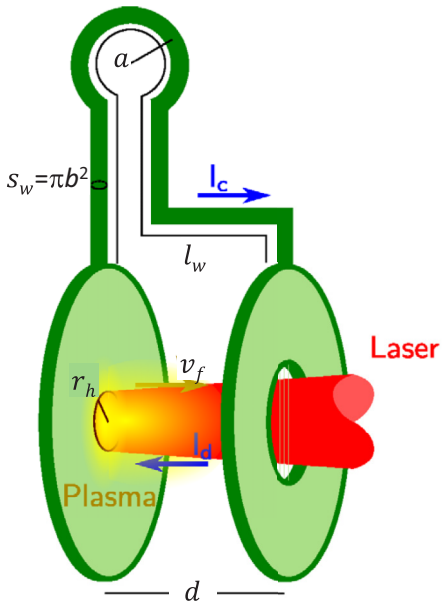


FIG. 1. Scheme of the capacitor coil target with notations used in the paper. The materials commonly used for target fabrication are aluminum, copper, nickel, and gold.

Apparently, there was a systematic error in the measurements, as that value corresponds to the energy stored in the magnetic field comparable to the laser pulse energy. These data were acquired with two diagnostics: the pickup magnetic coil and the optical Faraday rotation in a piece of glass placed near the target. Very likely, the measurement error is related to a poor knowledge of the Verdet constant of the glass sample irradiated by an x-ray flash from the laser spot.

These data were corrected in the subsequent experiment, carried out at the LULI2000 facility by Santos *et al.* [8], where magnetic fields up to 600 T were reported for a laser energy of 500 J but for a smaller coil of a diameter of 0.5 mm. There, the authors used laser intensities above $10^{17}$ W/cm$^2$ at the 1.06-$\mu$m wavelength, and magnetic B-dot probe measurements were compared with the data obtained from proton deflectometry. This was the first unambiguous measurement of the magnetic field in the coil, clearly separating it from the capacitor. However, the proton data were consistent with the B-dot measurements only at the raising part of the current, up to 350 ps, yielding a magnetic field of 100 T. The proton deflections have decreased at later times, which was explained by electrostatic screening the coil magnetic field by a plasma cloud emerging from the capacitor. This hypothesis was confirmed in a more recent experiment of the same group [9], where the proton radiography was obtained in the moment of the magnetic field maximum thanks for shielding of the coil from the diode. Figure 2 shows the magnetic fields measured with different diagnostic methods on the laser installations LULI2000 and GEKKO-XII.

All these data have, however, been collected in experiments with laser pulses of the energy less than 1 kJ and at wavelengths larger than 0.53 $\mu$m. Experiments in the domain of higher laser energies and shorter wavelengths of 0.35 $\mu$m were reported in Refs. [10,11]. The authors of Ref. [10] used two Omega EP laser beams with a total energy of 2.5 kJ in a 1-ns pulse and with an intensity $3 \times 10^{16}$ W/cm$^2$. The maximum magnetic field measured in the center of a U-shaped loop with a curvature radius of 0.3 mm was at the level of 40 T. The measurements were accomplished with two diagnostics: the B-dot probes and proton deflectometry. Moreover, by comparing the experiments with single and double loop coils the authors observed that the current in each coil remains the same. That is the signature of the laser diode operating as a *voltage source*, that is, the current in the circuit is inversely proportional to the external resistance, which has to be much larger than the internal resistivity of the diode itself. The efficiency of converting the laser pulse energy into the magnetic field in this experiment was about 0.01%, which is 10 times lower than the number reported in Ref. [6] and more than 100 times less than in Ref. [5]. This fact indicates a strong dependence of the coil-capacitor target performance on the laser wavelength. More efficient generation of magnetic field of 200 T on the same installation Omega EP and with a similar laser and target setup was reported recently [11].

A large scatter of the magnetic field measurements along with very basic qualitative estimates proposed in Refs. [4,5] gave rise to discussions concerning the quality of the collected data and the value of maximum current that can be delivered by a laser-driven diode [12]. In this paper we propose a more rigorous analysis of the capacitor-coil assembly operation and, in particular, an analysis of the performance of the laser-driven diode. In Sec. II we recall the initial model [5] and further improvements proposed in Refs. [11,12] and show their contradictions and limits. Then in Sec. III we propose a more physically justified model that accounts for major processes taking place during the laser pulse: the space charge neutralization, the plasma magnetization, and Ohmic heating of the coil wire. The major experimental results are recalled in Sec. IV and compared with the model. Section V contains our conclusions.

## II. MODEL OF A VOLTAGE SOURCE

### A. Simple model of the capacitor-coil system

A model of operation of the laser-driven capacitor-coil target was proposed in Refs. [4,5]. A simplified scheme with the corresponding notations is shown in Fig. 1. The tension $V_c$ at the coil edges is assumed to be given and the current $I_c$ in the external circuit is described by the equation

$$V_c = R_c I_c + L_c dI_c/dt, \tag{1}$$

where $R_c$ is the coil resistance and $L_c$ is its inductance. The magnetic field in the center of the coil $B_0$ is related to the current by the formula of the magnetic dipole, $B_0 = \mu_0 I_c/2a$, where $a$ is the coil radius and $\mu_0$ is the vacuum magnetic permeability. For the coil radius $a = 0.5$ mm, the current $I_c =$ 100 kA corresponds to the magnetic field of 125 T in the coil center. These numbers provide the reference point for our further estimates.

In order to estimate the current and tension, let us consider the following representative example of a copper target. The coil resistance $R_c = \eta l_w/s_w$ and inductance $L_c \simeq \mu_0 a \ln(a/b)$ depend on the wire length $l_w \simeq 2\pi a$, the cross section $s_w = \pi b^2$, and the wire radius $b$. The copper resistivity at the

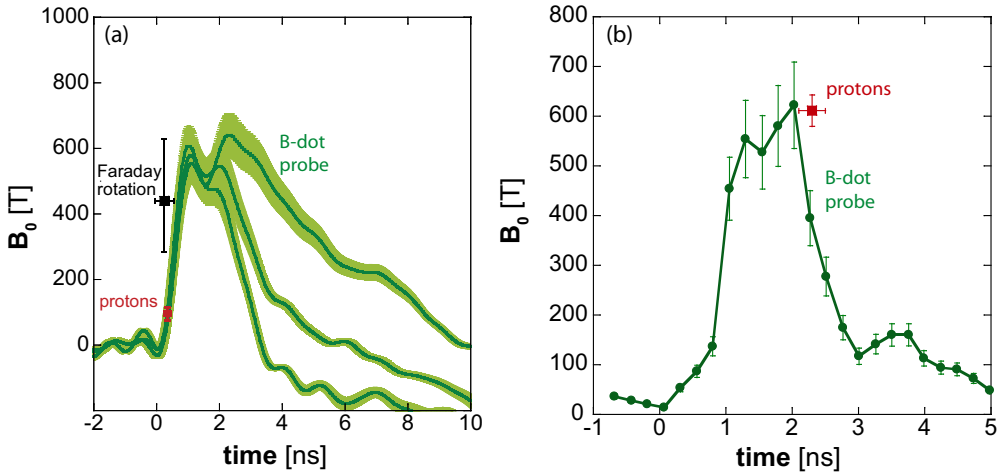


FIG. 2. Measurements of magnetic fields at the coil center of nickel targets with different diagnostics as reported in Refs. [8] (a) and [9] (b).

room temperature is $\eta_{\mathrm{Cu}} \simeq 2 \times 10^{-8}\ \Omega\,\mathrm{m}$. For $b \simeq 30\,\mu\mathrm{m}$ and $a = 1$ mm, the coil resistance is about 0.03 Ω and the inductance is $\sim 3$ nH. The corresponding relaxation time $\tau_c = L_c/R_c \sim 100$ ns is larger than the typical laser pulse duration, $t_{\mathrm{las}} \sim 1$ ns. That is, during the laser pulse, the inductance dominates and the coil current grows linearly with time, assuming a constant tension. Later in time when the capacitor is short cut and the laser is switched off, the current decreases exponentially with the relaxation time $\tau_c$. This behavior corresponds qualitatively to the observations presented in Ref. [5], although the relaxation time has to be corrected, accounting for the wire Ohmic heating. The value of the maximum tension generated in the diode is therefore defined by the laser pulse duration, $V_c \simeq L_c I_c / t_{\mathrm{las}} \sim 300$ kV.

The main problem is to explain the generation of such a high tension in the diode at the nanosecond time scale. The system is described in Refs. [5,6] as an empty capacitor with the capacitance $C_d = \epsilon_0 S_d/d$, where $\epsilon_0$ is the vacuum dielectric permittivity, $S_d \sim 10$ mm$^2$ the surface of the capacitor plate, and $d \simeq 1$ mm is the distance between the plates. The diode capacitance is very small, $C_d \simeq 0.1$ pF, so it can be rapidly charged to a high voltage even by a small current. Indeed, the tension of 300 kV in such a capacitor corresponds to the charge $Q_d = C_d V_c \sim 30$ nC. It could be charged with a 30-A current during the laser pulse time of 1 ns.

The charging current in the diode, $I_d$, is provided by emission of hot electrons from the laser-heated cathode. According to Ref. [5], these electrons are generated due to the resonance absorption of the laser pulse energy at the target surface. For the hot electron density $n_h$ and the distribution function $f_h$, the charging diode current is written as follows:

$$I_d = e\pi r_h^2 n_h \Delta\Omega \int_{eV_c}^{\infty} d\varepsilon\, v\, f_h(\varepsilon), \tag{2}$$

where $r_h$ is the radius of the emission zone, which can be assimilated to the radius of the laser spot; $\Delta\Omega$ is the solid angle of the hot electron emission; and $v$ and $\varepsilon$ are the electron velocity and kinetic energy. The low limit in the integral defines the minimum electron energy needed to access the anode having the potential $-V_c$. (We assume the cathode potential to be zero.) Then the diode tension is defined by the following relation:

$$C_d V_c = \int^t dt'\, I_d(t'). \tag{3}$$

By solving this relation one finds the tension $V_c(t)$, which then can be injected into Eq. (1) for calculation of the external current $I_c$. Similarly to the standard voltage source, the diode tension is independent of the external current and is defined by the internal process in the diode. Assuming a Maxwellian distribution of hot electrons with a temperature $T_h$ and electron emission in the solid angle $\Delta\Omega \sim \pi$ and replacing the time integration in Eq. (3) with a product of the characteristic current by the laser pulse duration, one obtains the following estimate for the diode potential:

$$eV_c \simeq T_h \ln\left(\frac{\omega_{ph}^2 t_{\mathrm{las}} d}{v_h}\frac{r_h^2}{S_d}\right), \tag{4}$$

where $\omega_{ph} = (e^2 n_h/\epsilon_0 m_e)^{1/2}$ is the plasma frequency associated with the hot electron density $n_h$ and $v_h = (T_h/m_e)^{1/2}$ is the hot electron thermal velocity. The term inside the logarithm can be easily of the order of $10^6$ or more, which corresponds to the tension of 15–20 times the hot electron temperature, $T_h$. So, for a modest hot electron temperature of 15–20 keV, one obtains a tension of the order of 200–300 kV, in good agreement with the observations.

However, these rapid estimates are oversimplified and contain a caveat, which has been missed by the authors of Refs. [5,6]. Indeed, the high ratio $eV_c/T_h \gtrsim 15$ implies a low current, $\lesssim$100 A, and a low charge in the capacitor, $Q_d \lesssim 100$ nC. In contrast, the high discharge current $I_c \sim 100$ kA transports during the same time a charge 1000 times larger. This strong charge imbalance is confirmed also by energy considerations: The estimated energy stored in the induction magnetic field in the coil is more than 1000 times larger than the electrostatic energy stored in the capacitor. A large energy needed to feed the coil current cannot be stored in the empty capacitor, and the separate analysis of the internal and external circuits leads to inconsistent results. Two solutions for this problem have been proposed: Either suppose that the system operates in a quasisteady regime, where a continuous charge flow through the diode is maintained by the laser pulse energy

deposition, or assume that the diode capacitance is much larger than estimated above. The first hypothesis proposed in Ref. [12] implies that the diode capacitance is small and the internal current is equal to the external current, $I_c = I_d$. The second hypothesis proposed in Ref. [11] implies that the capacitor is filled with a sufficiently dense plasma screening the electrostatic field.

According to Ref. [11], the capacitor is filled with a plasma produced by laser ablation from the cathode. Then the distance between the plates $d$ in the expression for the capacitance $C_d = \epsilon_0 S/d$ has to be replaced by the plasma Debye length $\lambda_D = (\epsilon_0 T_e/e^2 n_e)^{1/2}$, where $T_e$ and $n_e$ are the plasma temperature and density. The needed capacitance can be obtained assuming the ratio $d/\lambda_D$ to be of the order of $10^4$. This hypothesis unfortunately is not self-consistent: First, the needed plasma density is of the order of a few percentages of the critical density, so it would take a time of a few hundred picoseconds to fill the total capacitor volume, while the current is generated in a shorter time scale. Second, such a dense plasma would absorb incident laser radiation, thus reducing the energy flux to the cathode and thus the available current. Third, a large diode capacitance implies a large charging current, which cannot be larger than the discharge current. Then one should suppose that the charging and discharging currents are approximately equal, which brings us back to the first hypothesis. Fourth, such a dense plasma is a good conductor and it would short cut the circuit by providing the return current through the diode. As it is shown in the next section, the current continuity condition, $I_c = I_d$, can be satisfied without requiring a large diode capacitance.

### B. Plasma expansion from the cathode

The current continuity is an important propriety of the diode operation. Another important feature, already mentioned in the earlier paper [5], is the plasma expansion from the cathode under the energy deposited by the laser. The plasma isothermal expansion is described by the one-dimensional self-similar model [13–15]. The plasma density has an exponential spatial profile $n_h(z) = n_{h0}\exp(-z/c_s t)$ extending from the initial position $z = 0$ to the edge $z_f(t)$. Here $n_{h0}$ is the initial density of hot electrons, $c_s = (ZT_h/m_i)^{1/2}$ is the ion acoustic velocity, and $Z$ and $m_i$ are the ion charge state and mass. Position $z_f$ of the edge of expanding plasma is defined by the condition of quasineutrality; that is, the plasma local scale length $z_f$ has to be equal to the local Debye length $\lambda_D(z_f) = [\epsilon_0 T_h/e^2 n_h(z_f)]^{1/2}$. Solving the relation $\lambda_D(z_f) \simeq z_f$, one finds $z_f(t)$ and the plasma expansion velocity, $v_f = \dot{z}_f$:

$$z_f \simeq 2c_s t\ln(z_f/\lambda_{Dh}) \quad \text{and} \quad v_f \simeq 2c_s \ln(2c_s t/\lambda_{Dh}), \quad (5)$$

where $\lambda_{Dh} = (\epsilon_0 T_h/e^2 n_{h0})^{1/2}$ is the hot electron Debye radius. The expanding plasma is carrying an electric field $eE_z \simeq T_h/(c_s t)$. Multiplying this value by the plasma thickness $z_f$, one obtains the following expression for the potential drop in the diode: $eV_f \simeq -2T_h \ln(z_f/\lambda_{Dh})$. That is, the potential retaining the electrons at the cathode increases logarithmically with time, thus limiting the current flowing through the diode.

The authors of Ref. [12] proposed, however, another estimate for the potential drop in the diode $eV \sim -T_h d/(c_s t)$. This estimate could be obtained by multiplying the electric field $E_z$ by the distance between diode plates $d$. However, this cannot be the case, as the one-dimensional self-similar model is limited to short expansion times and to distances much smaller than the distance between the diode plates. As soon as the plasma size $z_f \simeq v_f t$ becomes comparable with the laser spot radius, $r_h$, the nonstationary planar plasma expansion transforms into a stationary spherical expansion, and the logarithmic time-dependent term in Eq. (5) has to be replaced by a constant value $\ln(r_h/\lambda_{Dh})$ [16]. Therefore, at the distance $z \sim r_h$ from the cathode the plasma expansion velocity and the potential jump are stabilized at the levels

$$v_m \simeq 2c_s \ln(r_h/\lambda_{Dh}) \quad \text{and} \quad eV_m \simeq -2T_h \ln(r_h/\lambda_{Dh}). \quad (6)$$

For the typical hot electron temperature $T_h \sim 20$–$40$ keV and the hot electron density $n_{h0} \sim 10^{21}$ cm$^{-3}$, the typical value of the ion acoustic velocity is $c_s \simeq 1$ mm/ns and the Debye length $\lambda_{Dh}$ is $\simeq 0.1\ \mu$m. Then for the typical value of the laser focal spot $r_h \lesssim 50\ \mu$m, the one-dimensional plasma expansion is limited to a narrow zone of less than 100 $\mu$m near the cathode, and the nonstationary expansion ends in less than 10 ps.

The important (but intermediary) conclusion following from that estimate is that ions at the edge of the planar expansion zone have already acquired a high velocity $v_f \simeq (10-15)c_s \simeq 10$–$15\ \mu$m/ps. That corresponds to the ratio of the ion energy to the hot electron temperature $\varepsilon_i/ZT_h \simeq 2\ln^2(r_h/\lambda_{Dh})$ which is of the order of 25–50. Assuming that the ion acceleration is stopped at the distance $r_h$ from the cathode, we conclude that the hot plasma arrives at the anode at the time $t_s \simeq d/v_f \sim 100$ ps, and after that moment the diode is operating in an approximately stationary regime throughout the laser pulse duration, which is of the order of 1 ns. Thus the diode is indeed filled with a tenuous plasma, while supplying the current in the external circuit.

## III. MODEL OF THE LASER DRIVEN DIODE

In this section we propose a model for the laser-driven diode operation that describes the electrostatic potential distribution inside the capacitor and the current that can be supplied to the external circuit. We start with the characterization of the laser-driven electron population, describe the potential distribution assuming a stationary operation, and then account for two complementary effects: the change of the parameters of the external circuit due to the Ohmic heating and magnetization of the current inside the diode.

### A. Hot electron characterization

The laser radiation interacting with the cathode plate generates hot electrons. In the intensity domain of interest, $I_{\rm las}\lambda_{\rm las}^2 \gtrsim 10^{14}$ W$\mu$m$^2$/cm$^2$, the major source of hot electrons is the laser resonance absorption. The theoretical analysis, numerical simulations, and comparison with experiments [17] suggest the following expressions for the density of hot electrons and their temperature:

$$n_{h0}/n_c \simeq 0.2\left(I_{\rm las}\lambda_{\rm las}^2/T_c\right)^{0.5}, \quad T_h \simeq 9\left(I_{\rm las}\lambda_{\rm las}^2\right)^{0.25}\ \text{keV}. \quad (7)$$

Here $n_c = 1.1\times 10^{21}\lambda_{\rm las}^{-2}$ cm$^{-3}$ is the electron critical density, $T_c$ is the temperature of the "cold" background plasma expressed in keV, the laser intensity $I_{\rm las}$ is expressed in the

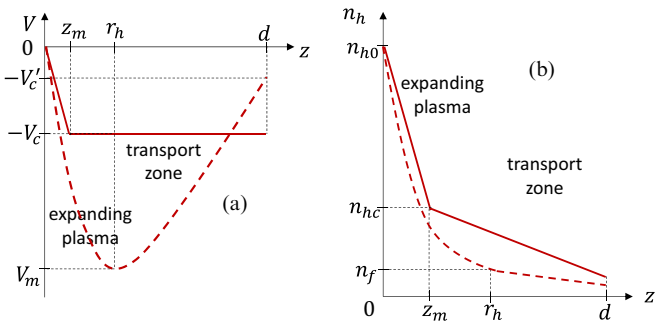


FIG. 3. Potential (a) and density (b) distribution in the diode. Stationary distribution is shown with solid lines, and dashed lines show the transient distribution before the potential equilibration.

units of PW/cm$^2$, and the laser wavelength $\lambda_{\rm las}$ is in microns. These expressions are valid, however, for the laser irradiances $I_{\rm las}\lambda_{\rm las}^2 \lesssim 10^{16}$ W$\mu$m$^2$/cm$^2$. According to the numerical simulations [18] and experimental measurements [19], the hot electron temperature scales for higher laser irradiances as

$$T_h \simeq 12\left(I_{\rm las}\lambda_{\rm las}^2\right)^{0.42}\,{\rm keV}, \tag{8}$$

where the units are the same as in Eq. (7). The correspondent hot electron density can be estimated by assuming a power balance, $hI_{\rm las} \simeq n_{h0}v_hT_h$, where $v_h = (T_h/m_e)^{1/2}$ is the hot electron average velocity and $h$ is the fraction of laser energy transferred to electrons. According to estimates presented in Ref. [11], it varies in the range from 0.01 to 0.1.

### B. Potential distribution in the diode

As it is explained in the previous section, the space inside the diode can be divided into two parts: (i) the plasma acceleration zone corresponding to a quasiplanar plasma expansion near the cathode, where the density decreases exponentially, and (ii) the transport zone corresponding to a quasispherical expansion at distances from the cathode larger than the laser focal spot size. A transition between these zones takes place at the distance $z \simeq r_h$, where the plasma density can be estimated as $n_f \simeq n_{h0}(\lambda_{Dh}/r_h)^2$. For the typical ratio $r_h/\lambda_{Dh} \sim 10^2$, the plasma density at the edge of the acceleration zone is already quite low, $n_f \lesssim 10^{-4}n_{h0}$, and the potential drop given by Eq. (6) exceeds the hot electron temperature already by a factor 10 or more. Assuming the cathode potential to be equal to zero and the hot electrons temperature $T_h \sim 20$ keV, the potential at the edge of acceleration zone $V_m$ would be of the order of $-200$ kV or more. The corresponding potential and density distributions are shown schematically in Fig. 3 by the dashed lines.

Knowing the plasma density and electron temperature, one can estimate also the value of the current in the diode. As it operates in a quasistationary regime, the current $I_d$ is the same at any position, and it can be evaluated at the edge of the zone of planar expansion $I_d' \simeq \pi r_h^2 e n_f v_h \simeq \pi\lambda_{Dh}^2 e n_{h0} v_h$. Thus, the electron current depends only on the hot electron temperature

$$I_d' \simeq \pi\epsilon_0 T_h v_h/e. \tag{9}$$

Estimating the diode impedance $Z_d' = V_f/I_d'$, one finds quite a large value:

$$Z_d' \simeq \frac{2}{\pi\epsilon_0 v_h}\ln\frac{r_h}{\lambda_{Dh}} = 240\,\Omega \times \frac{c}{v_{Th}}\ln\frac{r_h}{\lambda_{Dh}}. \tag{10}$$

It is evident that the diode impedance is two to three orders of magnitude larger than the impedance of the external circuit, and the laser-driven diode current is strongly limited by its internal impedance.

Such a configuration, however, cannot be stationary. Indeed, the potential at the anode $V_c$ is defined by the impedance of the external circuit, $Z_c \simeq R_c + L_c/t_{\rm las} \sim 1\,\Omega$. According to the hypothesis of a quasistationary diode operation, $I_d = I_c$, the absolute value of the anode tension $V_c' = Z_c I_d$ is much smaller than $|V_m|$. Therefore, the potential inside the diode has a deep minimum at $z \simeq r_h$. It decreases from zero value at the cathode to $V_m$ and then increases back to $V_c'$ in the transport zone $z > r_h$ (see dashed curves in Fig. 3). Consequently, the electric field in the diode changes sign and the ions accelerated in the zone of planar expansion would be decelerated in the transport zone. However, the plasma accumulation in the transport zone would then affect the potential distribution. It will evolve to reduce the ion overacceleration and make their distribution smoother. The only stationary configuration possible is the one corresponding to a monotonous profile of the electric potential and the ion velocity. It is shown in Fig. 3 by the solid lines: The potential drop in the plasma acceleration zone is connected to the anode with a plateau in the transport zone. Such a potential distribution is in agreement with the general theory of a plasma filled diode originally proposed by Pierce [20] and further developed in Refs. [21–23].

This configuration is the major result of our analysis: The potential at the end of the acceleration zone has to be equal to the anode potential, $-V_c = V_m$. The value of the potential jump $-V_c$ in the plasma acceleration zone is defined by the plasma distribution in the transport zone. The hot electron density decrease in the acceleration zone is limited by the value $n_{hc} = n_{h0}\exp(-eV_c/T_h)$ at the edge of the transport zone $z = z_m$, which is needed to maintain that potential jump. Then the electron current that is able to pass through that potential barrier can be estimated as $I_d \simeq e\pi r_h^2 n_{hc} v_h = I_0\exp[-eV_c(t)/T_h]$, where

$$I_0 \simeq e\pi r_h^2 n_{h0} v_h \tag{11}$$

defines the maximum current that can be extracted from the diode. According to the hot electron scaling (7), that value could be easily 10 MA or more. However, the current in the circuit is much smaller. It depends on the laser pulse duration and the impedance of the external circuit $Z_c$. The current-voltage characteristic of the diode is defined by the condition of the current continuity, $I_d = I_c$,

$$I_c(t) = I_0\exp[-eV_c(t)/T_h]. \tag{12}$$

For a crude estimate of the diode current, one can substitute the tension in the external circuit by a simplified relation, $V_c \sim Z_c I_c$. Solving then Eq. (12) in the limit $I_0 \gg T_h/eZ_c$ one finds:

$$I_c \simeq (T_h/eZ_c)\ln(eZ_cI_0/T_h). \tag{13}$$

Therefore, the dimensionless parameter controlling the diode current is $eZ_cI_0/T_h$. It can be easily of the order of $10^2$–$10^3$. That is, for the hot electron temperature $T_h \sim 30$–$40$ keV and the impedance of $Z_c \sim 1\,\Omega$, the tension in the diode could be of the order of $7\,T_h/e \simeq 200$ kV and the current of the order of 200 kA. That crude estimate shows a possibility to generate sufficiently high currents in a diode filled with a tenuous plasma. The potential distribution in our model is quite similar to the one proposed by the authors of Ref. [11], but the required plasma density in the diode is much lower, and the plasma fills not the whole volume between the anode and cathode but only the zone where current is transported. However, such a simplified model is not yet sufficient for applications. It does not account for such physical effects as the temporal evolution of the parameters of the external circuit and the magnetic field created in the diode.

### C. Time-dependent characteristics of the external circuit

Large currents flowing in the circuit induce the time variation of the coil parameters. The magnetic stress force $I_cBa \sim 10^5$–$10^6$ N acting on the coil with a mass $m_w \simeq 0.1$ mg corresponds to the displacement velocity $\sim 1-10\,\mu$m/ns, which is insufficient to change the coil shape. Therefore, the coil inductance can be considered as a constant. This estimate is in agreement with the conclusion of Ref. [11] based on the numerical modeling of the coil dynamics.

The Ohmic heating of the coil with the current of the order of 100 kA corresponds to the energy release of the order of 1 J, assuming the wire resistance of 0.1 Ω. In order to estimate the wire temperature, one should know the heat capacity of the copper $C_v = 0.385$ J/gK and the latent heat of the phase transitions melting and vaporization at the temperatures ∼1380 and 2860 K, respectively. The melting enthalpy $H_m \simeq 200$ J/g is relatively small, and it is sufficient to deliver 20 mJ to melt a wire with a mass of 0.1 mg. Heating to the vaporization temperature would require about 100 mJ. Both numbers are small compared to the expected energy release of 1 J. In contrast, the vaporization enthalpy $H_v \simeq 4600$ J/g is large, and the vaporization energy is comparable with the delivered energy. Therefore, one may expect the wire temperature to increase to the level of the order of vaporization temperature, which is approximately 3000 K, that is, 10 times the room temperature. The wire resistivity $\eta$ being linear function of the temperature is then increasing by a factor of 10 with respect to the estimate made in Sec. II A for a cold material. Similar arguments apply also to other materials, gold and nickel, used in the experiments [8,9,11].

The wire radial expansion also contributes to the wire temperature limitation. Shadowgraphic imaging of the coil during and after the laser pulse performed in the LULI2000 experiment [8] and shown in Fig. 4 indicates that the wire expands due to the Ohmic heating induced by the current. The wire radius increases with the velocity ∼11 $\mu$m/ns. The energy transmitted to the wire expansion can be estimated assuming that the velocity is increasing linearly with the radius. Then the wire kinetic energy can be written as $m_w v_w^2/8$, which is ∼1 J for the radial velocity $v_w \simeq 10\,\mu$m/ns. This estimate provides an additional argument for considering the figure of 3000 K as a reasonable estimate of the wire temperature.

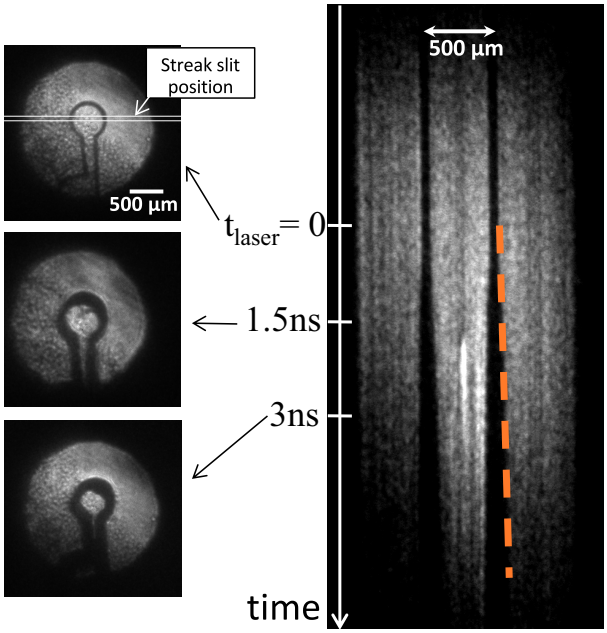


FIG. 4. Optical shadowgraphy (at 532 nm) of the coil expansion. On the left, 0.65-ns-gated images corresponding to a cold coil (top, $t = 0$) and two different timings after laser driving of the capacitor-coil target. On the right, the ns-scale expansion is resolved in a single shot by imaging the coil diameter into the slit of a streak camera. The average expansion velocity of the coil rod was measured to be $11 \pm 3\,\mu$m/ns (as indicated by the dashed orange line). Data acquired on the experimental campaign [8].

Another important issue is the skin effect. The nanosecond time scale of current variation is too short for a homogeneous distribution of the current in the wire. The current is localized in the skin layer of a thickness $l_s \simeq (\eta t_{\rm las}/\mu_0)^{1/2}$, which is of the order of 4 $\mu$m for a cold copper. This thickness is about 10 times less than the wire diameter. The current is thus localized at the wire surface leading to faster heating and surface ablation. However, as soon as the wire is heated to the temperature about 3000 K, the skin layer thickness is increasing by a factor of 3 and becomes comparable with the wire thickness. Therefore, for large currents corresponding to the maximum of magnetic field generation, the current distribution can be considered as sufficiently homogeneous in the wire. Nevertheless, the wire core remains cold, thus assuring the mechanical stability of the coil during the discharge time.

### D. Super-Alfvenic currents in the laser-driven diode

In the experiments with the laser-driven diode, the size of the laser spot at the cathode is rather small, of the order of 30–50 $\mu$m. This is necessary for obtaining a hot plasma and producing a large amount of energetic electrons. However, this size is more than 20–30 times smaller than the typical distance anode-cathode. Thus, the effects of transverse forces on the plasma dynamics and electric current have to be evaluated.

Let us consider the plasma in the transport zone inside the diode as a column with a given mass flow and a given electric current. Its radius $r_p$ is of the order of the laser

spot radius at the cathode, and it increases with the distance. According to the stationary model of the plasma expansion presented in Sec. III B, at the distance $z \sim r_h$ from the cathode, where the spherical expansion is formed, the hot electron density decreases to the level $n_{hc} \simeq n_{h0} \exp(-eV_c/T_h)$ and the ions are accelerated in the expanding plasma to the velocity $v_i \simeq c_s eV_c/T_h$, which is of the order of 3–5 mm/ns. The corresponding ion kinetic energy

$$\varepsilon_i = \frac{1}{2} m_i v_i^2 \simeq \frac{1}{2} Z T_h \left(\frac{eV_c}{T_h}\right)^2 \tag{14}$$

could attain the value of a few hundred keV, about 10 times larger than the hot electron temperature. We assume in what follows a constant axial ion velocity $v_i$ and a constant mass flow $\pi r_p^2 n_{hc} m_i v_i$.

As plasma propagates from the cathode to the anode its radius changes under the effect of two forces: the hot electron pressure gradient, $dP_e/dr$, and the Lorentz force, $\vec{j} \times \vec{B}$. Assuming a constant hot electron temperature and the maximum plasma density at the axis, the pressure gradient is directed toward the axis, thus creating a radial electric field, $E_r \simeq T_h/er_p$. This field induces a plasma expansion. Another contribution to the radial electric field is related to the electric current. The azimuthal magnetic field at the plasma edge can be estimated as $B_\theta \simeq \mu_0 I_d/2\pi r_p$. The radial Lorentz force $ev_h B_\theta$ acts on electrons pushing them towards the axis. That also corresponds to a radial electric field directed to the axis. The total radial electric field acting on ions can be estimated as a sum of these two contributions,

$$E_r \simeq -v_h B_\theta + T_h/er_p.$$

One can estimate the current needed to fully compensate the hot electron pressure from the force balance, $ev_h B_\theta \simeq T_h/r_p$. These two forces are equal, if $I_d \simeq I_A v_h/2c$, where $I_A = 4\pi m_e c/e\mu_0 = 17$ kA is the Alfven current. This condition does not depend on the plasma column radius. Consequently, super-Alfvenic currents are pinching the plasma column by pushing the ions towards the axis.

The evolution of the plasma radius with the distance inside diode can be estimated by assuming a small radial plasma velocity $v_r = dr_p/dt \ll v_i$. Combining then the equation for the ion acceleration $m_i dv_r/dt = ZeE_r$ with the relation for the ion axial displacement $dz = v_i dt$, one obtains an equation for the radius of plasma column in the following form:

$$\frac{d^2 r_p}{dz^2} \simeq -\frac{g}{r_p}, \quad \text{where} \quad g = \left(\frac{T_h}{eV_c}\right)^2 \left(2\frac{I_d c}{I_A v_h} - 1\right). \tag{15}$$

Two terms in the parenthesis in the expression for $g$ account for the Lorentz force and the electron pressure, respectively. The ion energy is related to the anode potential by Eq. (14). This equation can be integrated with the initial condition $dr_p/dz = \alpha_0$ near the cathode, $z \simeq z_m \ll d$, where $r_p = r_h$. Then we find a relation between the plasma divergence angle and the radius:

$$\left(\frac{dr_p}{dz}\right)^2 = \alpha_0^2 - 2g \ln \frac{r_p}{r_h}. \tag{16}$$

According to this equation, the plasma radius increases with the distance from cathode from the initial value $r_h$ at $z \simeq r_h$ to the maximum value $r_{\max} = r_h \exp(\alpha_0^2/2g)$ and then decreases back to zero. The value $r_p = 0$ corresponds to the collapse of the plasma column. The distance where the collapse takes place corresponds to the maximum distance of the current transport. The collapse length $z_{\text{coll}}$ is defined by the integral of Eq. (16):

$$z_{\text{coll}} = r_h \int_0^{\exp(\alpha_0^2/2g)} \frac{dx}{\sqrt{\alpha_0^2 - 2g \ln x}}.$$

Equating the collapse distance to the distance between the diode plates, we find a condition for the maximum current that can be transported through the diode:

$$\sqrt{2g/\pi} = (r_h/d) \exp\left(\alpha_0^2/2g\right). \tag{17}$$

This equation relates the coefficient $g$ (15) to the geometric characteristics of the diode: the plasma flow divergence $\alpha_0$ and the ratio $d/r_h$. In the domain parameters of interest $\alpha_0 \lesssim 2$ and $d/r_h \lesssim 20$ this function is shown in Fig. 5. It increases with the plasma divergence and decreases with the diode width remaining below 1 in the whole domain. Considering now the definition of $g$ in Eq. (15), we find then the expression for the maximum diode current:

$$I_p \simeq 0.5 I_A \frac{v_h}{c}\left[1 + g\left(\frac{eV_c}{T_h}\right)^2\right]. \tag{18}$$

The maximum diode current is thus a quadratic function of the tension. In the domain of low tensions, $eV_c \lesssim T_h$, it is limited by the Alfven current. For high tensions, $eV_c > T_h$, the maximum current can be increased above this value if the coefficient $g$ is sufficiently large. By increasing the initial plasma divergence $\alpha_0$, one may significantly increase the maximum current. For example, for $d/r_h = 10$ the coefficient $g$ increases from 0.03 for $\alpha_0 = 0$ to 1 for $\alpha_0 = 2$.

Thus, while the current magnetization imposes a limitation on the maximum current, it may exceed several times the Alfven current in the considered geometry. The crucial parameters in that relation are the ratio of the electrostatic potential to the hot electron temperature and the plasma stream divergence. By increasing these parameters, one enforces the rigidity of the plasma flow and, correspondingly, its capacity to transport larger electron currents.

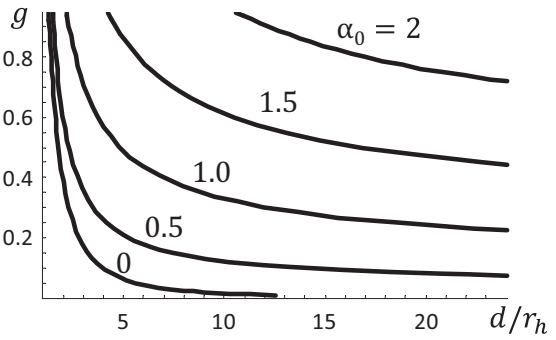


FIG. 5. Dependence of the parameter $g$ on the plasma flow divergence $\alpha_0$ and the ratio $d/r_h$ according to Eq. (17). The values of $\alpha_0$ are shown with numbers near the correspondent curves.

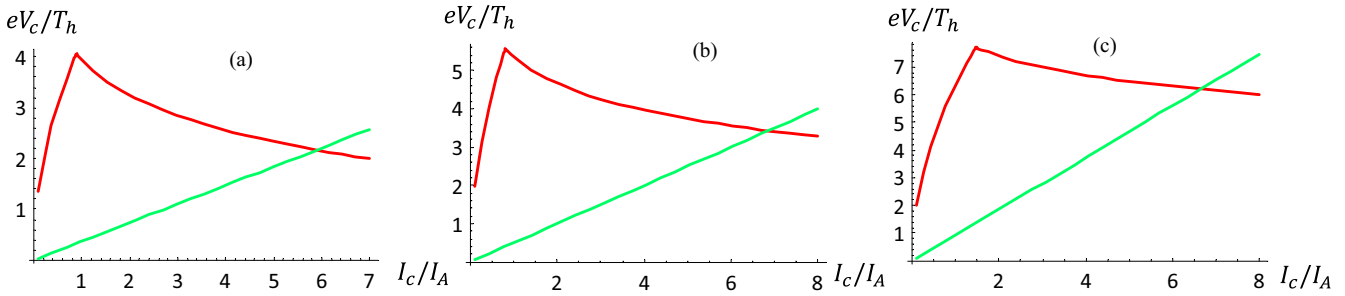


FIG. 6. Current-voltage characteristic of the diode $V_c(I)$ accounting for the effects of the space charge and magnetization. The chosen set of parameters corresponds to the experiments [5] (a), [6] (b), and [10] (c). The distance between the diode plates is set to 1 mm and the resistance $R_c = 1\ \Omega$.

## IV. DISCUSSION

### A. Current-voltage characteristic

Combining the current-voltage characteristics related to the space charge limit (12) $I_{sc}(V_c)$ and the plasma magnetization (18) $I_{pm}(V_c)$, we can define the diode current-voltage characteristic as a minimum between these two limitations: $I_c(V_c) = \min\{I_{sc}, I_{pm}\}$. Examples of such characteristics are shown in Fig. 6 for the conditions corresponding to the experiments [5,6,10]. The curves corresponding to the limits (12) and (18) (neglecting the term 1 in the square brackets) are shown by the red lines and the green lines correspond to the coil Ohm's law, $V_c = R_c I_c$, with the resistance $R_c$ set to 1 Ω. It delimits the maximum current that can be achieved in the circuit.

Two curves $I_{pm}(V_c)$ and $I_{sc}(V_c)$ cross at the current value $I_*$. The magnetization limits the diode tension for the currents smaller than $I_*$. This part of the characteristic $I_c < I_*$ corresponds to the normal differential resistance $dV_c/dI_c > 0$. The maximum tension where $I_c = I_*$ can be estimated by the following expression:

$$eV_{max} \simeq T_h \ln(2I_0 c/I_A v_h). \tag{19}$$

Typically, $I_*$ is of the order of the Alfven current and $V_{max}$ is a few times larger than the hot electron temperature. For $I_c > I_*$ the diode current is limited by the cathode potential jump. Three panels in Fig. 6 show the variation of the current generation conditions in function of the laser intensity and wavelength. In the experiment [5] [Fig. 6(a)] a $CO_2$ laser at the wavelength $\lambda_{las} = 10.6\ \mu$m was delivering to a copper target a 100-J pulse of 1-ns duration to a focal spot of $r_h = 120\ \mu$m. The intensity of $1.3 \times 10^{14}$ W/cm$^2$ corresponds to the hot electron temperature of 40 keV and the hot electron density $n_{h0}/n_c \simeq 0.1$. The model shows that the maximum tension is expected to be about $4T_h$, that is, 160 kV, and the maximum current could attain $6I_A$, that is, 100 kA. However, because of the laser pulse duration shorter than the relaxation time $\tau_c \sim 10$ ns, the current is limited to about 40–50 kA. These numbers are in qualitative agreement with the measurements.

In the experiment [6] [Fig. 6(b)], a Nd glass laser at the wavelength $\lambda_{las} = 1.05\ \mu$m was delivering to a copper target a 300-J pulse of 1-ns duration to a focal spot of $r_h = 30\ \mu$m. The intensity of $\sim 10^{16}$ W/cm$^2$ corresponds to the hot electron temperature of 30 keV and the hot electron density $n_{h0}/n_c \simeq 0.07$. The model shows that the maximum tension is expected to be about $5T_h$, that is, 150 kV, and the maximum current could attain $6I_A$, that is, 100 kA. However, because of a short laser pulse duration and a relatively large coil inductance of ~4 nH, the current is limited to about $1.3I_A$, that is, 20 kA. These numbers are also in qualitative agreement with the measurements.

In the experiment [10] [Fig. 6(c)] two 1 ns laser beams at the third harmonic of a Nd glass laser at the wavelength $\lambda_{las} = 0.35\ \mu$m were delivering 2500 J to a focal spot of $r_h = 60\ \mu$m. The intensity of $\sim 2 \times 10^{16}$ W/cm$^2$ corresponds to the hot electron temperature of 18 keV and the hot electron density $n_{h0}/n_c \simeq 0.045$. The model shows that the maximum tension is expected to be about $7T_h$, that is, 120 kV, and the maximum current could attain $6I_A$, that is, 100 kA. However, because of a short laser pulse duration and a relatively large coil inductance of ~2 nH, the current is limited to about $1.6I_A$, that is, 30 kA. These numbers are also in qualitative agreement with the measurements.

A quantitative comparison would require us to account for the temporal laser pulse profile, the coil heating, resistivity evolution, and other factors. The present model is aiming at a qualitative evaluation of the major physical processes in the diode and a possible optimization of its performance. Figure 6 demonstrates the validity of our model for a large domain of laser wavelengths and intensities.

### B. Temporal profile of the diode current

Knowing the current-voltage characteristic one can solve the external circuit equation (1) and find the temporal profile of the current that can be achieved in the coil. Figure 7 shows the temporal profiles of the current in the coil and the tension for the parameters of the experiment by Santos *et al.* [8]. Here, the laser pulse at the wavelength $\lambda_{las} = 1.05\ \mu$m of energy 500 J and duration 1 ns was delivered to a nickel target at the focal spot of a radius $a = 15\ \mu$m achieving intensity of $\sim 10^{17}$ W/cm$^2$. The coil inductance is 2 nH, the resistance of a cold wire is 0.1 Ω and the distance between diode plates is 0.85 mm. The corresponding hot electron temperature is 84 keV and $n_{h0}/n_c \simeq 0.22$. In that simulation, the coil resistance was increased to $R_c = 1\ \Omega$ accounting for the wire heating as discussed in Sec. III C. The corresponding relaxation time $\tau_c = L_c/R_c \simeq 2$ ns is twice longer than the laser pulse duration.

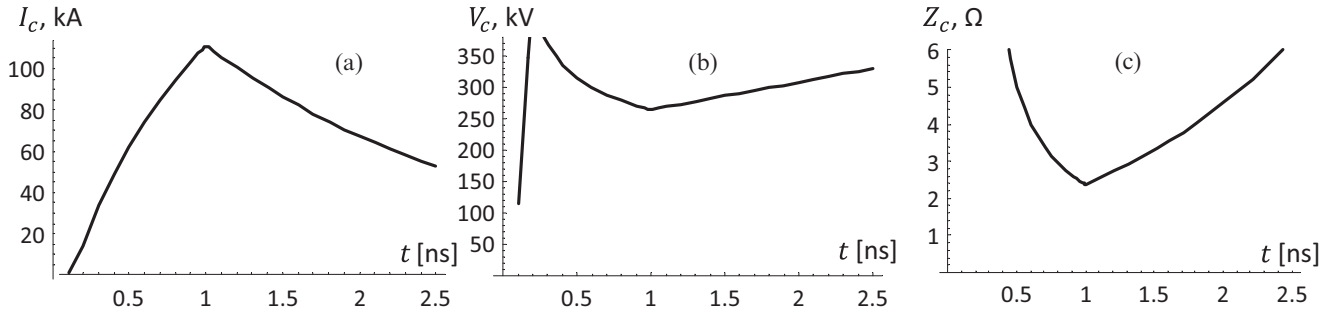


FIG. 7. Temporal dependence of the current $I_c$ (a) and tension (b) in the diode-coil circuit (a) and the circuit impedance $Z_c = V_c/I_c$ (c). The parameters correspond to the experiment [8].

The current shown in Fig. 7(a) continuously grows with time, attaining the value of 110 kA at the end of the laser pulse. It is smaller than the value of 250–300 kA claimed in [8], but that difference is acceptable due to the model simplifications. The tension stays approximately constant at the level ∼300 kV, which corresponds to the regime of current limitation by the cathode potential jump. The circuit impedance is decreasing with time approaching the value of the coil resistance, which was maintained constant in the present model. According to Eq. (13), the dimensionless parameter controlling the current saturation in this regime is the ratio of the hot electron temperature to the product of the coil impedance to the maximum diode current, $T_h/eZ_cI_0$. So the current can be further increased by increasing the hot electron temperature, that is, the laser irradiance, $I_{las}\lambda_{las}^2$, and the impedance of the external circuit. The former implies increasing the laser pulse energy as the intensity is already defined.

## V. CONCLUSIONS

The analysis of capacitor-coil system presented in this paper allows us to identify its mode of operation and the major parameters controlling the current intensity and duration. Considering this system as an electric circuit, we conclude that the optimal regime is achieved if the internal and external impedances are comparable, and with a nanosecond laser pulse the diode operates in the quasistationary regime because of its small capacitance. The diode operation time can be optimized by adjusting three characteristic times: the laser pulse duration, the response time of the external circuit (corrected by the effect of Ohmic heating), and the time of plasma propagation through the diode. The latter one depends on the ratio of the size of the laser focal spot and the distance between the capacitor plates.

The important point is the time delay in the discharge current, which is equal to the time needed for fast ions to propagate through the diode. It is demonstrated that the charge accumulation in the Debye sheath limits the vacuum diode current to a low value, and only neutral plasma is capable to maintain large electron currents for a sufficiently long time. The maximum diode tension for the diode current smaller than the Alfven current is limited by the current magnetization. The higher diode currents are limited by the internal impedance of the diode. The present model neglects physical effects related to the cold plasma expansion from the cathode and anode and the return current in the diode if the plasma density increases. Analysis of these effects is out of the scope of the paper. They appear on a time scale of a few nanoseconds and may eventually short cut the current in the external circuit.

The maximum current delivered by the diode is proportional to the hot electron temperature. The major control parameter is the laser irradiance $I_{las}\lambda_{las}^2$. The use of high laser intensities (tight focusing) and long wavelengths may improve the diode performance, providing more energetic electrons capable of maintaining a high current at large potential jumps. The capacitor-coil setup is limited to the currents in the range up to a few hundred kiloamperes and to durations of a few nanoseconds. A systematic experimental study of the system performance in function of the laser intensity and capacitor geometry is desirable for comparison with the theoretical model. It would be also desirable to measure the plasma characteristics inside the diode, to verify the plasma neutrality, and to measure its density, the magnetic fields, and the energies of ions accelerated in the cathode sheath.

## ACKNOWLEDGMENTS

This work has been carried out within the framework of the EUROfusion Consortium and has received funding from the Euratom research and training programme 2014-2018 under Grant No. 633053. The views and opinions expressed herein do not necessarily reflect those of the European Commission. We also acknowledge financial support from the French National Research Agency (ANR) in the framework of "the investments for the future" Programme IdEx Bordeaux-LAPHIA (Grant No. ANR-10-IDEX-03-02).

[1] B. B. Pollock, D. H. Froula, P. F. Davis, J. S. Ross, S. Fulkerson, J. Bower, J. Satariano, D. Price, K. Krushelnick, and S. H. Glenzer, High magnetic field generation for laser-plasma experiments, Rev. Sci. Instr. **77**, 114703 (2006).

[2] B. Albertazzi, J. Béard, A. Ciardi, T. Vinci, J. Albrecht, J. Billette, T. Burris-Mog, S. N. Chen, D. Da Silva, S. Dittrich, T. Herrmannsdórfer, B. Hirardin, F. Kroll, M. Nakatsutsumi, S. Nitsche, C. Riconda, L. Romagnagni, H.-P. Schlenvoigt,

S. Simond, E. Veuillot, T. E. Cowan, O. Portugall, H. Pépin, and J. Fuchs, Production of large volume, strongly magnetized laser-produced plasmas by use of pulsed external magnetic fields, Rev. Sci. Instr. **84**, 043505 (2013).

[3] V. V. Korobkin and S. L. Motylev, On a possibility of using laser radiation for generation of strong magnetic fields, Sov. Tech. Phys. Lett. **5**, 474 (1979).

[4] J. F. Seely, Pulsed megagauss fields produced by laser-driven coils, Appl. Phys. B **31**, 37 (1983).

[5] H. Daido F. Miki, K. Mima, M. Fujita, K. Sawai, H. Fujita, Y. Kitagawa, S. Nakai, and C. Yamanaka, Generation of a Strong Magnetic Field by an Intense $CO_2$ Laser Pulse, Phys. Rev. Lett. **56**, 846 (1986).

[6] C. Courtois, A. D. Ash, D. M. Chambers, R. A. D. Grundy, and N. C. Woolsey, Creation of a uniform high magnetic-field strength environment for laser-driven experiments, J. Appl. Phys. **98**, 054913 (2005).

[7] S. Fujioka Z. Zhang, K. Ishihara, K. Shigemori, Y. Hironaka, T. Johzaki, A. Sunahara, N. Yamamoto, H. Nakashima, T. Watanabe, H. Shiraga, H. Nishimura, and H. Azechi, Kilotesla magnetic field due to a capacitor-coil target driven by high power laser, Sci. Rep. **3**, 1170 (2013).

[8] J. J. Santos, M. Bailly-Grandvaux, L. Giuffrida, P. Forestier-Colleoni, S. Fujioka, Z. Zhang, P. Korneev, R. Bouillaud, S. Dorard, D. Batani, M. Chevrot, J. E. Cross, R. Crowston, J.-L. Dubois, J. Gazave, G. Gregori, E. d'Humiéres, S. Hulin, K. Ishihara, S. Kojima, E. Loyez, J.-R. Marqués, A. Morace, P. Nicolaï, O. Peyrusse, A. Poyé, D. Raffestin, J. Ribolzi, M. Roth, G. Schaumann, F. Serres, V. T. Tikhonchuk, P. Vacar, and N. Woolsey, Laser-driven platform for generation and characterization of strong quasi-static magnetic fields, New J. Phys. **17**, 083051 (2015).

[9] K. F. F. Law, M. Bailly-Grandvaux, A. Morace, S. Sakata, K. Matsuo, S. Kojima, S. Lee, X. Vaisseau, Y. Arikawa, A. Yogo, K. Kondo, Z. Zhang, C. Bellei, J. J. Santos, S. Fujioka, and H. Azechi, Direct measurement of kilo-tesla level magnetic field generated with laser-driven capacitor-coil target by proton deflectometry, Appl. Phys. Lett. **108**, 091104 (2016).

[10] L. Gao, H. Ji, G. Fiksel, W. Fox, M. Evans, and N. Alfonso, Ultrafast proton radiography of the magnetic fields generated by a laser-driven coil current, Phys. Plasmas **23**, 043106 (2016).

[11] C. Goyon, B. B. Pollock, D. P. Turnbull, A. Hazi, L. Divol, W. A. Farmer, D. Haberberger, J. Javedani, A. J. Johnson, A. Kemp, M. C. Levy, B. Grant Logan, D. A. Mariscal, O. L. Landen, S. Patankar, J. S. Ross, A. M. Rubenchik, G. F. Swadling, G. J. Williams, S. Fujioka, K. F. F. Law, and J. D. Moody, Ultrafast probing of magnetic field growth inside a laser-driven solenoid, Phys. Rev. E **95**, 033208 (2017).

[12] G. Fiksel, W. Fox, L. Gao, and H. Ji, A simple model for estimating a magnetic field in laser-driven coils, Appl. Phys. Lett. **109**, 134103 (2016).

[13] A. V. Gurevich, L. V. Pariiskaya, and L. P. Pitaevskii, Ion acceleration upon expansion of a rarefied plasma, Sov. Phys. JETP **36**, 274 (1973).

[14] P. Mora, Plasma Expansion into a Vacuum, Phys. Rev. Lett. **90**, 185002 (2003).

[15] V. Yu. Bychenkov, V. N. Novikov, D. Batani, V. T. Tikhonchuk, and S. G. Bochkarev, Ion acceleration in expanding multispecies plasmas, Phys. Plasmas **11**, 3242 (2004).

[16] L. Robson, P. T. Simpson, R. J. Clarke, K. W. D. Ledingham, F. Lindau, O. Lundh, T. McCanny, P. Mora, D. Neely, C.-G. Wahlström, M. Zepf, and P. McKenna, Scaling of proton acceleration driven by petawatt-laser-plasma interactions, Nat. Phys. **3**, 58 (2007).

[17] D. W. Forslund, J. M. Kindel, and K. Lee, Theory of Hot-Electron Spectra at High Laser Intensity, Phys. Rev. Lett. **39**, 284 (1977).

[18] K. Estabrook and W. L. Kruer, Properties of Resonantly Heated Electron Distributions, Phys. Rev. Lett. **40**, 42 (1978).

[19] W. Priedhorsky, D. Lier, R. Day, and D. Gerke, Hard X-ray Measurements of 10.6$\mu$m Laser-Irradiated Targets, Phys. Rev. Lett. **47**, 1661 (1981).

[20] J. R. Pierce, Limiting stable current in electrons beams in the presence of ions, J. Appl. Phys. **15**, 721 (1944).

[21] P. L. Auer, Potential distributions in a low-pressure thermionic converter, J. Appl. Phys. **31**, 2096 (1960).

[22] R. G. McIntyre, Extended space-charge theory of low-pressure thermionic converters, J. Appl. Phys. **33**, 2485 (1962).

[23] S. Kuhn, Axial equilibria, disruptive effects, and Buneman instability in collisionless single-ended Q-machines, Plasma Phys. **23**, 881 (1981).